



This is a repository copy of *General design rules for space harmonic cancellation in multiphase machines with multiple converters and star-polygonal windings.*

White Rose Research Online URL for this paper:

<https://eprints.whiterose.ac.uk/214283/>

Version: Accepted Version

---

**Article:**

Rudden, I., Li, G.-J. [orcid.org/0000-0002-5956-4033](https://orcid.org/0000-0002-5956-4033), Zhu, Z.Q. et al. (3 more authors) (2024) General design rules for space harmonic cancellation in multiphase machines with multiple converters and star-polygonal windings. IEEE Transactions on Energy Conversion. ISSN 0885-8969

<https://doi.org/10.1109/TEC.2024.3422611>

---

© 2024 The Authors. Except as otherwise noted, this author-accepted version of a journal article published in IEEE Transactions on Energy Conversion is made available via the University of Sheffield Research Publications and Copyright Policy under the terms of the Creative Commons Attribution 4.0 International License (CC-BY 4.0), which permits unrestricted use, distribution and reproduction in any medium, provided the original work is properly cited. To view a copy of this licence, visit <http://creativecommons.org/licenses/by/4.0/>

**Reuse**

This article is distributed under the terms of the Creative Commons Attribution (CC BY) licence. This licence allows you to distribute, remix, tweak, and build upon the work, even commercially, as long as you credit the authors for the original work. More information and the full terms of the licence here: <https://creativecommons.org/licenses/>

**Takedown**

If you consider content in White Rose Research Online to be in breach of UK law, please notify us by emailing [eprints@whiterose.ac.uk](mailto:eprints@whiterose.ac.uk) including the URL of the record and the reason for the withdrawal request.



[eprints@whiterose.ac.uk](mailto:eprints@whiterose.ac.uk)  
<https://eprints.whiterose.ac.uk/>

# General Design Rules for Space Harmonic Cancellation in Multiphase Machines with Multiple Converters and Star-Polygonal Windings

I. A. Rudden<sup>1</sup>, G. J. Li<sup>1</sup>, *Senior Member, IEEE*, Z. Q. Zhu<sup>1</sup>, *Fellow, IEEE*, A. Duke<sup>2</sup>, R. Clark<sup>2</sup>, and A. Thomas<sup>2</sup>

<sup>1</sup>, Department of Electronic and Electrical Engineering, The University of Sheffield, Sheffield, UK

<sup>2</sup>, Siemens Gamesa Renewable Energy Limited, North Campus, Broad Lane, Sheffield, UK

[g.li@sheffield.ac.uk](mailto:g.li@sheffield.ac.uk).

**Abstract**--This paper presents a general rule for the design of  $m$ -phase machines supplied by  $n$ -converters that employ a hybrid star-polygonal winding in each  $m$ -phase set. This rule shows that for any  $m$ -phase machine supplied by  $n$ -converters, there exists a set of feasible slot-pole numbers in conjunction with the star-polygonal connection that allows for optimum winding MMF harmonic performance. This also allows for tables of feasible solutions to be generated, including coil pitch and calculated winding factors. From this, the star of slots method is used to obtain the winding layout of any feasible machine for comparison of its winding MMF harmonic performance. An example 3-phase machine is investigated and a number of trends for all  $m$ -phase  $n$ -converter machines can be identified. In machines with a coil pitch of 1, excellent harmonic elimination is observed for all non-torque producing harmonics and machine performance is all-round enhanced. A prototype machine has been manufactured and EMF and static torque measurements validate the predictions.

**Index Terms**-- Concentrated windings, fractional-slot, harmonics, multiphase machine, star-delta.

## I. INTRODUCTION

There is an increasing reliance on high performance electrical machines in the modern world due to a rapidly growing renewable energy market and transition to electrification of transport [1]. This has led to a wealth of research in numerous machine topologies, optimization strategies, and general design rules for electrical machines to fit certain purposes. One topology that has gained increasing popularity over the last twenty years is machines equipped with Fractional Slot Concentrated Windings (FSCW) [2]. These machines differ from the conventional Integer Slot Distributed Windings (ISW) in that they have a number of slots per pole per phase of less than one, in contrast to the ISW machines where this value is often an integer. This allows for a multitude of slot-pole combinations in FSCW that can be chosen to meet specific requirements. For example, a 3-phase ISW machine with 12-slots must have 2 or 4 poles, whereas a 3-phase FSCW with 12-slots is likely to have 10 or 14 poles but could differ even from that [3]. These machines offer many potential advantages over their ISW counterparts including higher torque capability, lower torque ripple, greater ease of manufacture, and higher fault tolerance [4]. However, one substantial downside of FSCW machines is unfortunately the presence of a larger number of unwanted or ‘parasitic’ harmonics in the winding magnetomotive force (MMF) [5]. These harmonics come about due to the concentrated nature of the coils when compared with distributed windings that are overlapped, thus creating a more sinusoidal winding MMF. Unwanted harmonics in FSCW

machines lead to increases in rotor losses, particularly eddy current losses in PMs, as they rotate asynchronously with the rotor [6, 7]. This can be problematic as the rotor is often harder to cool than the stator and large PM eddy current losses excessively heat the PMs leading to thermal demagnetization. As this is clearly undesirable there are several strategies often employed to reduce these unwanted MMF harmonics in PM machines including stator shifting and multilayer windings [8, 9]. In wound-field (WF) machines, the armature MMF harmonics also induce unwanted EMF harmonics in the excitation windings caused by the mutual inductance between the coils. These lead to torque instability and increase torque ripple and losses [10, 11].

Another strategy that can be used to minimize unwanted harmonics is the use of multiphase machines. Owing to the prevalence of 3-phase systems, Zhu *et al* categorized multiphase machines into two broad camps: multi-three-phase machines and other multiphase machines in [12]. As the name suggests, multi-three phase machines employ a number of phases that are some integer multiple of three, such as 6 or 9 phases. These can also be described as dual or triple 3-phase machines and so on, owing to the number of converters used in their operation. Dual 3-phase machines have been studied extensively in numerous works and offer many benefits over conventional machines such as: higher fault tolerance, improved electromagnetic torque, and higher efficiency [13, 14]. Many of these benefits are a consequence of the ability for a dual 3-phase machine to eliminate unwanted parasitic harmonics in the winding MMF and improve the amplitude of the working harmonic. These methods can be applied to both PM machines [15] and WF machines [16, 17]. Other multiphase machines, as defined by Zhu *et al*, are machines using several phases that are not a multiple of 3, such as 5- or 7-phase machines. These types of machines are generally less common than 3-phase machines, however still offer many benefits over 3-phase machines such as higher output torque with reduced torque ripple, higher efficiency, and higher fault tolerance [18]. However, these benefits do come at an increased cost and complexity of both the machine and converter used in their operation.

One technique that mimics the performance of a multiphase machine is to use a hybrid star-polygonal winding technique instead of a second converter in a dual  $m$ -phase machine. The polygonal shape depends on the number of phases and as example is often referred to as a delta or pentagon winding in 3- and 5-phase machines respectively. The groundwork for this is laid out in [19] wherein it is demonstrated that star-polygonal windings can be used to mimic the performance of a dual  $m$ -phase machine while still

only using one converter. This work is extended in [20] where a detailed analysis of the harmonic MMF elimination in  $m$ -phase star-polygonal wound machines is carried out. The star-polygonal winding connection has been thoroughly studied in literature including comparisons of different star-polygonal winding topologies [21, 22], and novel machines [23, 24]. It has thus far been shown that the winding MMF harmonic performance of a machine can be improved with the addition of more converters, using a number of phases beyond 3, and using a hybrid star-delta connection to mimic a multiphase machine. It stands to reason that the cumulative effect of these techniques could result in even greater improvement of a machine's winding MMF harmonic performance.

In [25] a dual 3-phase machine that employs star-delta windings is proposed that performs better than a conventional dual 3-phase machine, and in [26] multiple 3-phase machines with star-delta windings are investigated and compared. These works show the cumulative benefit of multiple 3-phase machines employing star-delta windings, however only machines with coil pitches above 1 are studied in detail and experimentally. Furthermore, the possible machine topologies for multi-phase machines with star-polygonal windings has not been covered (such as 5- or 7-phases). Thus, this paper sets out to define the general rule under which any  $m$ -phase machine supplied by  $n$ -converters can be effectively wound with star-polygonal coils to improve machine performance and reduce unwanted harmonics. Once this rule is established, feasible slot-pole number combinations are calculated for any machine with  $m$ -phases,  $n$ -converters, varying coil pitches, and star-polygonal windings. From this, the harmonic performance of various machines is investigated, and some cases are presented in this work. While the theory of this paper is applicable to any  $m$ -phase  $n$ -converter machine, a particular focus is applied to 3- and 5-phase machines with only up to four converters for simplicity. It is found that machines designed using this process exhibit excellent harmonic MMF cancellation properties in addition to increasing the amplitude of torque producing harmonics. This will result in machines with improved torque performance, reduced rotor losses, and higher efficiency.

## II. WINDING THEORY

### A. Star-Polygonal windings

The underlying work on space harmonic cancellation in machines with star-delta wound fractional slot concentrated windings is outlined in [19]. In this work Abdel-Khalik *et al* demonstrated that for a general  $m$ -phase machine with star and polygonal windings displaced by one slot and connected as shown in Fig. 1(a) the corresponding phasor diagram for winding MMF shown in Fig. 1(b) is achieved.

This machine configuration utilizes the relative phase shift of currents in a polygonal winding compared to a star winding

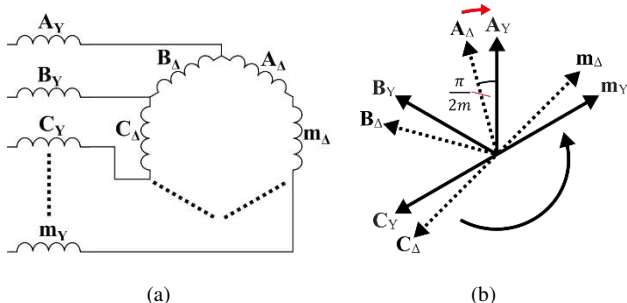


Fig. 1.  $m$ -phase star-polygonal machine design. (a) Winding layout of star and polygonal coils, and (b) corresponding coil phasor diagram.

to bring coils that would normally be slightly out of phase to being perfectly in-phase. Currents in a polygonal winding are shifted by  $\pi/2m$  relative to a star winding, so by appropriately matching adjacent coils in electrical space and winding them either in star or in a polygonal shape, they can be brought in-phase as shown by the red arrow in Fig. 1(b). Thus, machines with star-polygonal windings are often able to achieve a distribution factor of one. At the same time, this phase shift can also suppress or even eliminate unwanted harmonics in the winding MMF. In [19] this harmonic elimination is demonstrated on a common 12s/10p 3-phase machine to simulate the performance of a split-phase machine. The winding layouts and comparison of the winding MMF harmonics between a conventional star winding and the hybrid star-delta winding can be seen in Fig. 2. There is a difference in the magnitude of current in star and polygonal connected windings, thus the number of turns in the polygonal connected coils are adjusted appropriately using

$$N_{\Delta} = 2 \sin \frac{\pi}{m} N_Y \quad (1)$$

where  $N_Y$  is the number of turns in a star coil. As mentioned previously, the star-polygonal winding mimics the behavior of a dual  $m$ -phase machine wound conventionally and being operated with two converters. Thus, it stands to reason that in machines where additional converters are used to drive independent star-delta winding sets, a cumulative 'stacking' of phase shifts of numerous coils can be used to improve the distribution factor of the working harmonic in such machines, in addition to eliminating even more unwanted harmonics.

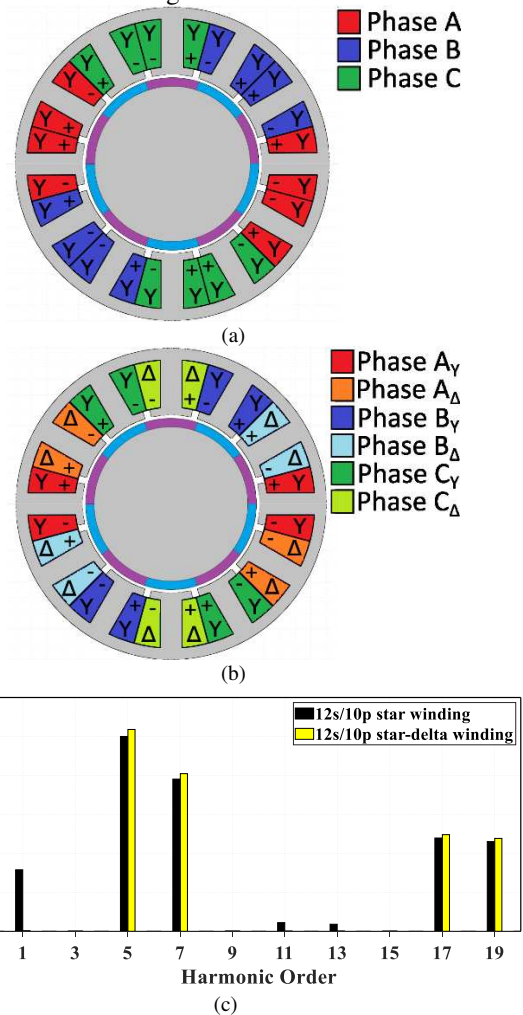


Fig. 2. Comparison of 3-phase 12s/10p machines. (a) Conventional star winding, (b) star-delta winding, and (c) armature MMF harmonics.

### B. $m$ -Phase $n$ -Converter Machines

In a conventional  $2m$ -phase machine the electrical angle between phases is given by

$$\alpha = \frac{2\pi}{2m} \quad (2)$$

For a split-phase machine, the phase-belt of a conventional  $2m$ -phase winding is split into two halves with the phase separation between the two  $m$ -phase winding sets being given by

$$\beta = \frac{\alpha}{2} = \frac{\pi}{2m} \quad (3)$$

where  $\beta$  is the electrical space phase separation between two  $m$ -phase winding sets in a split-phase machine and  $\alpha$  is the angle between phases in a conventional  $2m$ -phase machine.

This means that for a machine of this type to be feasible, the angle between any two successive slots must equal  $\beta$ . It can then be observed that this corresponds to machines having a number of slots equal to  $4m$  or its multiples. When introducing  $n$  additional converters, the phase-belt of the winding must be split once more by the number of converters introduced. This gives the required electrical angle ( $\sigma$ ) between the  $n$ -converter  $m$ -phase winding sets as

$$\sigma = \frac{\beta}{n} = \frac{\pi}{2mn} \quad (4)$$

Again, this corresponds to a rule dictating a feasible number of slots – in this case  $N_s = 4mn$  or its multiples. The phase angle between coils in electrical space is a function of the slot-pole number combination of any machine. Thus, it is possible to formulate all feasible slot-pole number combinations that allow for an  $m$ -phase  $n$ -converter machine to employ star-polygonal windings given a required electrical angle and slot number. For this machine to be feasible, each coil must occupy a unique position in electrical space. This allows the phasors for the working harmonic to be brought in-phase by the unique and cumulative impact of both converter and star-polygonal windings as shown in Fig. 3.

To calculate the electrical angle between coil phasors for any slot-pole number combination, the combined sum of all adjacent coil angles must be divided by the total number of coils. For a double-layer winding the total number of coils is equivalent to the slot number. This is known as a Gaussian Summation and can be used to obtain the electrical angle between each adjacent coil.

$$\theta_e = 2 \times \left( \pi - \frac{\sum_{k=0}^{N_s} \text{mod}(kp\theta_m, 2\pi)}{N_s} \right) \quad (5)$$

where  $p$  is the pole pair number, and  $\theta_m$  is the mechanical slot pitch. For any  $m$ -phase  $n$ -converter machine to employ star-polygonal windings the electrical space vector angle  $\theta_e$  must

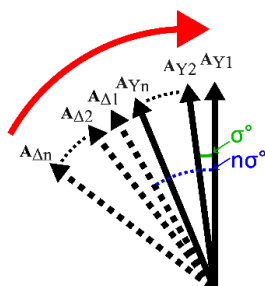


Fig. 3. Phasor diagram for Phase A in an  $m$ -phase  $n$ -converter star-polygonal wound machine.

equal the required angle  $\sigma$ . In this case, each of the coil space vectors must occupy a unique position in electrical space. This means that the Gaussian sum of their electrical angles must be equal to  $(N_s - 1)\pi$ . As such, (5) can be rewritten purely in terms of  $m$ ,  $n$ , and  $p$  to give a criterion that must be met for any  $m$ -phase  $n$ -converter machine with  $2p$  poles to be feasible

$$\sum_{k=0}^{4mn} \text{mod}\left(\frac{kp\pi}{2mn}, 2\pi\right) = \pi(4mn - 1) \quad (6)$$

Using this equation, it is possible to quickly iterate through all pole-numbers and identify cases where this rule is true. Therefore, a table of all feasible slot-pole number machines can be created for any  $m$ -phase  $n$ -converter machine and is demonstrated in the following section.

### III. ANALYTICAL MODEL OF WINDING MMF

#### A. Generating Feasible Solutions

A process was set up to determine all feasible pole number solutions for an  $m$ -phase  $n$ -converter machine with star-polygonal windings following the theory outlined in section II. A flowchart describing this process can be seen in Fig. 4. This process can then be applied to any  $m$ -phase  $n$ -converter machines. As example, it has been applied to a dual 3-phase 24-slot machine, and the results are shown in Fig. 5. Values up to  $2p = N_s$  have been plotted to demonstrate the symmetry of feasible machines of this type. However, solutions past  $2p = N_s + 2$  can be ignored as at this point increasing the pole number begins to cause a drop in the pitch factor. Therefore, only solutions that lie in the region indicated by the  $2p < N_s + 2$  region will be considered. From this work, tables can be generated for  $m$ -phase machines with varying numbers of converters. The winding factor ( $K_w$ ) of an electrical machine is the sum of the pitch ( $K_p$ ) and distribution factor ( $K_d$ ) given by

$$K_w = K_p K_d \quad (7)$$

For all these machines, the distribution factor is unity as demonstrated by the phasor diagram in Fig. 1(b). This means that the winding factor is simply equal to the pitch factor given by

$$K_p = \cos(\gamma/2) \quad (8)$$

where  $\gamma$  is the difference in span angle (elec. deg.) between the coil and the pole pitches. To achieve the highest possible pitch factor,  $\gamma$  should be minimized and this can be done by adjusting the coil pitch of each machine. The optimum coil pitch for each slot-pole multiple to maximize the pitch factor can be found by simply dividing the slot-number by the pole-number and rounding to the nearest integer value. The potential slot-pole number combinations for 3-phase star-delta wound machines with up to 4 converters is given in TABLE I as well as their calculated winding factors and associated coil pitches. As evidenced in this table, it is possible to generate a 3-phase machine employing star-delta windings using many different converter numbers and coil pitches. Traditionally one of the main advantages of the FSCW machines is the concentrated nature of the windings, so a coil-pitch of one is likely the most desired. However, in many cases specific pole number will be required in which case it is worth being aware of the possible winding factors and coil pitches for such a pole number, depending on the number of converters used.

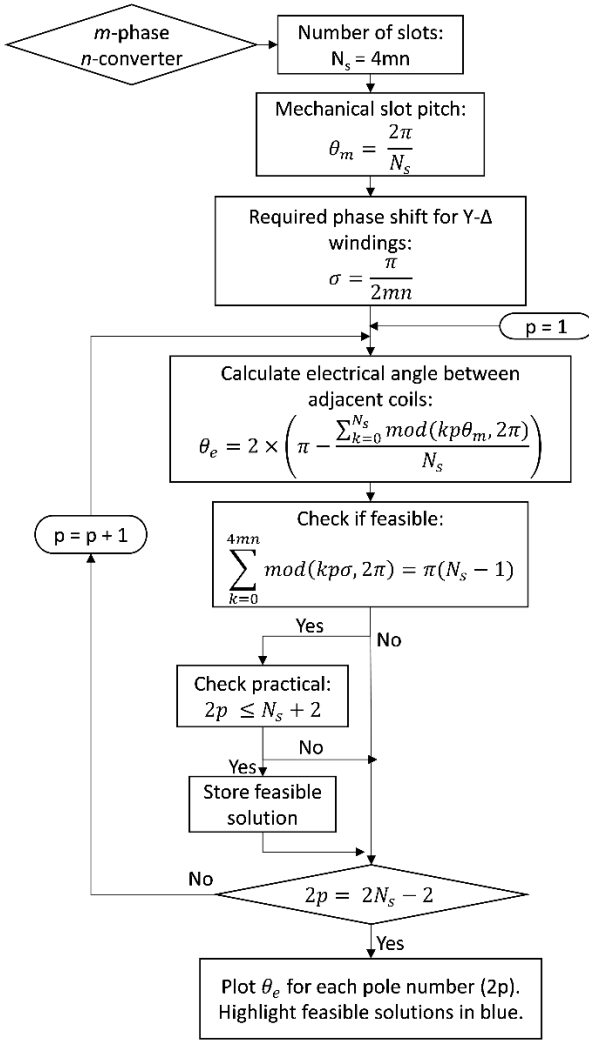


Fig. 4. Flowchart showing the process for obtaining feasible solutions.

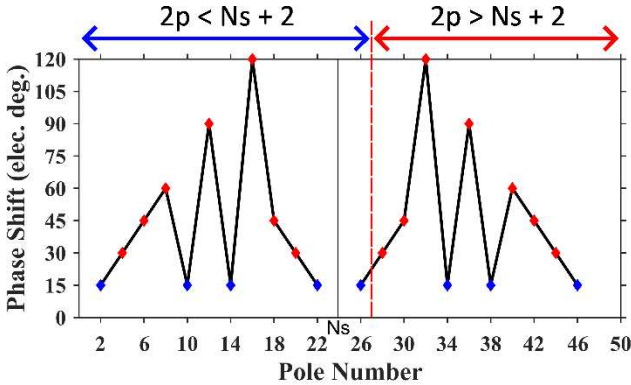


Fig. 5. Phase shift between coils in 24-slot, 2-converter 3-phase machine with varying pole numbers. Slot-pole number combinations that satisfy equation (6) are highlighted in blue, and those that do not satisfy this equation are highlighted in red.

TABLE I WINDING FACTORS OF POSSIBLE 3-PHASE  $n$ -CONVERTER MACHINES WITH STAR-DELTA WINDINGS.

$2p$	$N_s$			
	12 ( $n=1$ )	24 ( $n=2$ )	36 ( $n=3$ )	48 ( $n=4$ )
2	1.0 (6)	1.0 (12)	1.0 (12)	1.0 (12)
10	0.966 (1)	0.966 (2)	0.985 (4)	0.998 (5)
14	0.966 (1)	0.966 (2)	0.966 (3)	0.981 (3)
22	-	0.991 (1)	0.940 (2)	0.991 (2)
26	-	0.991 (1)	0.906 (1)	0.991 (2)
34	-	-	0.996 (1)	0.897 (1)
38	-	-	0.996 (1)	0.947 (1)
46	-	-	-	0.998 (1)
50	-	-	-	0.998 (1)

Note: coil pitch of each machine included in brackets.

## B. $m$ -Phase Rotating Fields

The method described in Section III.A produces feasible solutions by considering slot-pole number combination, but it overlooks whether a balanced  $m$ -phase winding creates a magnetic field that rotates synchronously with the chosen pole number. Therefore, it is necessary to compute the harmonic order and rotation direction of all magnetic fields induced in the air-gap by the windings. Any slot-pole number combination with a pole pair number that doesn't align with the harmonic orders of the field generated by the  $m$ -phase winding must be discarded. The harmonic order and rotation direction of all fields rotating in the air-gap can be ascertained by investigating the composition of the MMF time and space contents of an  $m$ -phase winding from its individual phase windings. Firstly, assuming the windings carry a peak AC current of  $\sqrt{2}I_c$  at a frequency of  $\omega = 2\pi f$ , then the MMF magnitude for the  $h^{\text{th}}$  harmonic is

$$|F_h| = \frac{4H}{h\pi} \times K_{wh} \quad (9)$$

where  $K_{wh}$  is the winding factor for the  $h^{\text{th}}$  order harmonic and  $H = \frac{N_c i(t)}{2p}$  with  $i(t) = \sqrt{2}I_c \sin \omega t$  and  $h = 1, 3, 5, \dots$ . Therefore, the resultant time and space content of the single-phase winding MMF can be calculated using

$$F(\theta, t) = [F_1 \sin(\theta) + \dots + F_h \sin(h\theta)] \sin(\omega t) \quad (10)$$

where  $\theta$  is the angle around the machine in mech. deg. Using trigonometric identities, this can then be altered to give

$$F(\theta, t) = \frac{F_1}{2} [\cos(\theta - \omega t) - \cos(\theta + \omega t)] + \dots + \frac{F_h}{2} [\cos(h\theta - \omega t) - \cos(h\theta + \omega t)] \quad (11)$$

Here it can be seen that each harmonic order produces fields that rotate in the positive direction ( $h\theta - \omega t$ ) and fields that rotate in the negative direction ( $h\theta + \omega t$ ). In an  $m$ -phase winding each phase is displaced by  $2\pi/m$  elec. deg. This means that the time and space content for any  $h^{\text{th}}$  harmonic in any  $\varphi^{\text{th}}$  phase (with reference to the first) can be calculated using the general equation (13). This equation can then be broken down into forward and backward rotating field components based on the positive or negative sign for  $\omega t$ . By summing the resultant MMF for a chosen harmonics' forward or backward rotating components across all  $m$ -phases, the existence of a field can be determined. These equations are given in (14). For any  $h^{\text{th}}$  harmonic the resultant field will equal zero when there is no field rotating for that harmonic either forward or backward. This derivation applies to machines with balanced  $m$ -phase windings where  $m$  is odd, requiring a symmetric winding layout. As it has already been highlighted that a star-polygonal machine must have a number of slots equal to  $4mn$  or its multiples this criterion is already met. Using these equations, the existing fields and their direction for any balanced  $m$ -phase machine can be observed and some examples are shown in TABLE II. From TABLE II it can be seen that for a balanced  $m$ -phase machine, the existing fields follow a specific rule such as

$$h = 2mk \pm 1 \quad (12)$$

where  $k$  is any integer and fields of the order  $2mk+1$  rotate synchronously with the fundamental (or first order harmonic) and fields of the order  $2mk-1$  rotate in the reverse direction to the fundamental.

TABLE II HARMONIC FIELD COMPONENTS IN BALANCED  $m$ -PHASE MACHINES

$m$	Fields
3	1,-5,7,-11,13,-17,19...
5	1,-9,11,-19,21,-29,31...
7	1,-13,15,-27,29,-41,43...
...	...
$m$	$h = 2mk \pm 1$

Note: a negative sign before the order dictates a field rotating in opposite direction to the fundamental.

TABLE III WINDING FACTORS AND COIL PITCHES FOR FEASIBLE 5-PHASE  $n$ -CONVERTER MACHINES WITH STAR-PENTAGON WINDINGS

$2p$	$N_s$	$40$			
		$(n=1)$	$(n=2)$	$(n=3)$	$(n=4)$
2	20	1.0 (10)	1.0 (20)	1.0 (30)	1.0 (40)
6	20	0.988 (3)	0.997 (7)	-	0.999 (13)
14	20	0.891 (1)	0.997 (3)	0.995 (4)	0.997 (6)
18	20	0.988 (1)	0.988 (2)	-	0.988 (4)
22	20	0.988 (1)	0.988 (2)	0.988 (3)	0.988 (4)
26	20	-	0.891 (2)	0.978 (2)	0.999 (3)
34	20	-	0.972 (1)	0.978 (2)	0.972 (2)
38	20	-	0.997 (1)	0.914 (2)	0.997 (2)
42	20	-	0.997 (1)	-	0.997 (2)
46	20	-	-	0.934 (1)	0.972 (2)
54	20	-	-	-	0.872 (1)
58	20	-	-	0.999 (1)	0.908 (1)
62	20	-	-	0.999 (1)	0.938 (1)
66	20	-	-	-	0.962 (1)
74	20	-	-	-	0.993 (1)
78	20	-	-	-	0.999 (1)
82	20	-	-	-	0.999 (1)

With this new rule in mind, the possible slot-pole number combinations for  $m$ -phase machines with  $n$ -converters to employ star-polygonal windings must be reassessed. As an example, the feasible slot-pole solutions for a 5-phase machine are given in TABLE III. This table shows all feasible slot-pole number combinations according to the process outlined in Section AIII A. However, only the rows highlighted in green remain feasible when the existence of rotating fields is taken into account. With the tables of feasible solutions for any  $m$ -phase  $n$ -converter machine updated it is then possible to generate the winding structure for each topology to investigate the harmonic performance.

### C. Creating Winding Layouts

To measure the harmonic performance of star-polygonal windings in each  $m$ -phase  $n$ -converter machine the armature MMF must be plotted. To do this, the winding layout must first be worked out and this is done using the common star of slots methodology outlined in [27]. The breakdown for applying this process in the case of  $m$ -phase  $n$ -converter

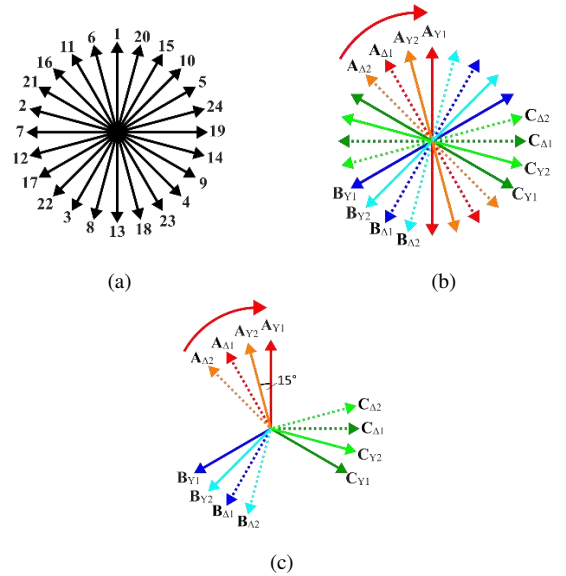


Fig. 6. Star of slots method for arranging coils into star-delta windings and 2<sup>nd</sup> converter for a dual 3-phase machine. (a) Initial electrical phase angles of all coils, (b) coils identified depending on phase, winding type, and converter, and (c) reversible coils flipped to produce final phasor diagram.

machines is outlined below with a diagram representation in Fig. 6, where a 24s/10p dual 3-phase machine is used as an example:

- (1) The first coil is used as a reference for 0 elec. deg. This coil is taken to be the phase A star coil in the first converter.
- (2) Using this coil as a reference, the electrical phase angle of every other coil is calculated.
- (3) Coils in each phase are then identified as being shifted by integer multiples of  $2\pi/\varphi$  elec. deg. from phase A.
- (4) The star coils in each subsequent converter are identified by how many integer multiples of  $\sigma$  they are shifted from the star coils in the first converter.
- (5) The polygonal connected coils are then identified in each  $i^{\text{th}}$  converter as being shifted by  $n \times i \times \sigma$  elec. deg. from their respective phase star winding, where  $n$  is the total number of converters.
- (6) Finally, all coils that are phase shifted by 180 elec. deg. from coils identified thus far are noted as needing reversing to be brought in-phase.

With the star of slots for any winding layout obtained, it is possible to plot the winding MMF of each machine to investigate the harmonic performance. Based on the work in [19] the MMF field generated by any star or polygonal connected coil in an  $m$ -phase,  $n$ -converter star-polygonal wound machine is given by (15) and (16) where  $\varphi$  and  $j$

$$F_{\varphi n} = \frac{F_n}{2} \left[ \cos \left( h\theta - \frac{2h\pi(\varphi-1)}{m} - \left( \omega t - \frac{2\pi(\varphi-1)}{m} \right) \right) - \cos \left( h\theta - \frac{2h\pi(\varphi-1)}{m} + \left( \omega t - \frac{2\pi(\varphi-1)}{m} \right) \right) \right] \quad (13)$$

$$\begin{cases} F_{n-fwd} = \frac{mF_n}{2} \sum_{\varphi=1}^m \cos \left( h\theta - \frac{2h\pi(\varphi-1)}{m} - \left( \omega t - \frac{2\pi(\varphi-1)}{m} \right) \right) \\ F_{n-bck} = \frac{mF_n}{2} \sum_{\varphi=1}^m \cos \left( h\theta - \frac{2h\pi(\varphi-1)}{m} + \left( \omega t - \frac{2\pi(\varphi-1)}{m} \right) \right) \end{cases} \quad (14)$$

where  $\varphi$  defines the different phase numbers within the machine.

$$F_{mnY}(\theta, t) = \sum_{h=2mk \pm 1}^{\infty} \frac{4mN_{cY}I_m}{h\pi} \sin \left( \frac{h\pi}{4m} \right) \cos \left( h(\theta - \theta_{mech}) + \sigma(j-1) - \omega t - \frac{2\pi(\varphi-1)}{m} \right) \cos \left( \omega t - \frac{2\pi(\varphi-1)}{m} \right) \quad (15)$$

$$F_{mn\Delta}(\theta, t) = \sum_{h=2mk \pm 1}^{\infty} \frac{4mN_{c\Delta}I_m}{h\pi} \sin \left( \frac{h\pi}{4m} \right) \cos \left( h(\theta - \theta_{mech}) + \beta + \sigma(j-1) - \omega t - \frac{2\pi(\varphi-1)}{m} \right) \cos \left( \omega t - \frac{2\pi(\varphi-1)}{m} \right) \quad (16)$$

correspond to the  $\varphi^{\text{th}}$  and  $j^{\text{th}}$  phase number and converter number in the machine respectively,  $N_{cY}$  is the number of turns in the star wound coils and  $N_{c\Delta}$  is the number of turns in the polygonal connected coils, and  $I_m$  is the rms phase current. If a coil is reversed, the result is multiplied by -1. With this process established, it is possible to investigate the harmonic performance of all feasible  $m$ -phase  $n$ -converter machines with star-polygonal windings. Some topologies are investigated in the following section that give a general overview of this expected performance.

#### D. Harmonic Performance

As evident in TABLE I and TABLE III, there are multiple feasible slot-pole number combinations for star-polygonal wound machines with  $m$ -phases and  $n$ -converters that retain the advantageous of a coil pitch of 1. The simplest of these to investigate are the 3-phase, 2-converter, 24s/22p machine and the 5-phase, 2-converter, 40s/38p machine. After running this slot-pole number combination through the process outlined in section III, the following winding layouts shown in Fig. 7 are obtained. To assess the harmonic elimination performance of these split-phase winding layouts, the winding MMFs for both a conventional 3-phase 24s/22p machine and a dual 3-phase 24s/22p machine with star-delta windings have been plotted and compared in Fig. 8. Here, the MMFs for a conventional 5-phase 40s/38p machine and a dual 5-phase 40s/38p machine with star-pentagon windings are also displayed.

It can be seen that the proposed winding layouts successfully eliminate a number of unwanted winding MMF harmonics in addition to an increase in the primary working harmonic. It has been demonstrated in [28, 29] that for fractional slot machines, armature MMFs of the order  $|p \pm jN_s|$  (where  $p$  is the rotor pole-pair number,  $N_s$  is the number of slots, and  $j$  is any integer) are modulated by the stator teeth and thus become torque producing. Therefore, in the 3-phase machine both the 11<sup>th</sup> and 13<sup>th</sup> harmonics are torque producing and have both been enhanced by this winding design. Similarly, for the 5-phase machine, both the 19<sup>th</sup> and 21<sup>st</sup> harmonics are torque producing and have been enhanced by this winding design. TABLE IV shows a breakdown of the impact the proposed topology has on each specific harmonic.

The increase by 4.4% for the 3-phase machine and 1.5% for the 5-phase machine in the amplitudes of both harmonics where  $2h = N_s \pm 2$  offers huge benefit to torque production. However, the amplitude increase exhibited by the 5-phase machine is substantially lower when compared to the 3-phase machine. This is a trend that continues in machines with higher phase number and so the benefit of employing star-polygonal windings reduces as well [19]. Furthermore, the number of parasitic harmonics in machines with higher phase numbers is inherently lower. Thus, the harmonic elimination benefit of this winding layout also decreases as the number of phases increases, as shown in Fig. 8. To assist in understanding the composite effect of the dual 3-phase machine and star-delta windings on harmonic performance, as well as validate the analytical results in this section the 24s/22p machine was modelled in FEA. The machine was then configured as a single 3-phase machine, dual 3-phase machine with 15 elec. deg. phase shift between the two converters, single 3-phase machine with star-delta windings, and then a dual 3-phase machine with star delta windings. In each case the windings were excited with sinusoidal current

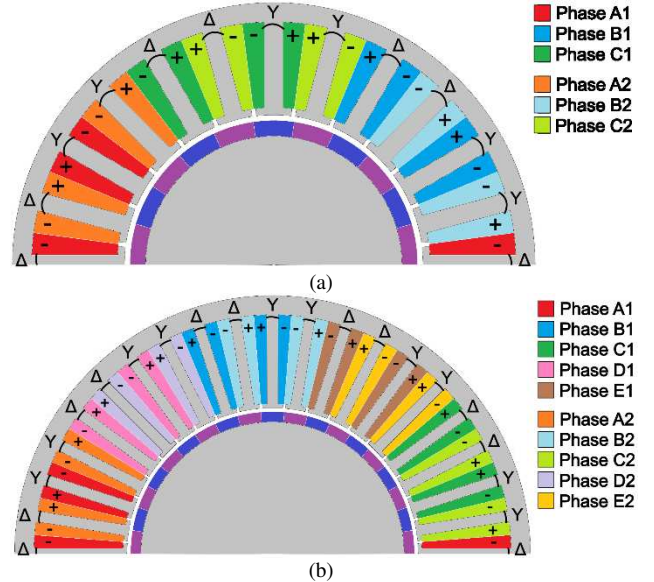


Fig. 7. Winding layout for dual  $m$ -phase machines with star-polygonal windings (a) 24s/22p 3-phase and (b) 40s/38p 5-phase. Only half the machine is displayed due to winding symmetry.

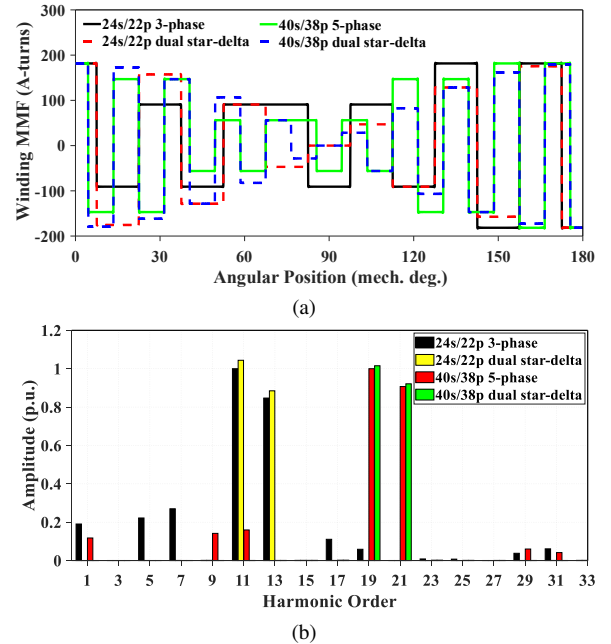


Fig. 8. Comparison between  $m$ -phase machines and dual  $m$ -phase star-polygonal wound machines (a) Winding MMF and (b) harmonic spectra with amplitude taken in per unit using the single  $m$ -phase working harmonic as reference.

TABLE IV MAGNITUDE OF HARMONICS IN 24S/22P MACHINES

Harmonic Order	24s/22p 3-phase	24s/22p dual star-delta
1 <sup>st</sup>	0.191	0 (-100%)
5 <sup>th</sup>	0.222	0 (-100%)
7 <sup>th</sup>	0.270	0 (-100%)
11 <sup>th</sup>	1.0	1.044 (+4.4%)
13 <sup>th</sup>	0.848	0.885 (+4.4%)
17 <sup>th</sup>	0.111	0 (-100%)
19 <sup>th</sup>	0.0593	0 (-100%)

TABLE V MAGNITUDE OF HARMONICS IN 40S/38P MACHINES

Harmonic Order	40s/38p 5-phase	40s/38p dual star-pentagon
1 <sup>st</sup>	0.117	0 (-100%)
9 <sup>th</sup>	0.141	0 (-100%)
11 <sup>th</sup>	0.159	0 (-100%)
19 <sup>th</sup>	1.0	1.012 (+1.5%)
21 <sup>st</sup>	0.904	0.885 (+1.5%)
29 <sup>th</sup>	0.0600	0 (-100%)
31 <sup>st</sup>	0.00415	0 (-100%)

and the flux density in the air-gap are obtained numerically, the results are comparatively plotted in Fig. 9.

It can be seen that the dual 3-phase machine successfully eliminates the 1<sup>st</sup> subharmonic when compared to the 24s/22p 3-phase machine. The star-delta windings successfully eliminate the 5<sup>th</sup>, 7<sup>th</sup>, 17<sup>th</sup>, and 19<sup>th</sup> harmonics such that the composite effect of the dual star-delta windings yields total harmonic elimination of all but the 11<sup>th</sup> and 13<sup>th</sup> harmonics. Additionally, the amplitudes of the torque producing flux density harmonics are both increased by 4.5% which is in close agreement with the analytical result. To better understand the behavior (increase or reduction) of each harmonic, the respective winding MMF phasor diagrams for the 3-phase machine are shown in Fig. 10. These phasor diagrams serve as a graphical vector representation of the sinusoidal nature of the armature MMF. They show that when the phasors align with one another there is harmonic superposition and the magnitude of this harmonic is enhanced. When the phasors are shifted by 180° with respect to each other the sinusoidal MMFs of that harmonic are perfectly anti-phase and so completely eliminate one another. This cancellation occurs because the peaks of one wave align with the troughs of the other, resulting in a net zero effect on the MMF. It can be seen that the star-delta windings work to eliminate the 5<sup>th</sup>, 7<sup>th</sup>, 17<sup>th</sup>, and 19<sup>th</sup> harmonics. The second converter, operating at a 15 elec. deg. phase shift serves to eliminate the 1<sup>st</sup> subharmonic. The phasors for the 11<sup>th</sup> and 13<sup>th</sup> harmonic line up such that neither harmonic is eliminated by this structure, and in fact both are enhanced. The increase by 4.5% in the torque producing harmonics, coupled with the successful elimination of several parasitic harmonics make this machine topology an attractive option for improving machine performance. Especially as this topology maintains a coil pitch of 1, and so the lower end winding losses and ease of manufacture inherent to a FSCW are maintained. The same is true for the 5-phase machine, with phasor diagrams being omitted for brevity. It is worth noting that this relation between  $m$ -phase  $n$ -converter machines and the increase in harmonics of the order  $2h = N_s \pm 2$  while successfully eliminating practically all other harmonics remains true for all  $m$ -phase  $n$ -converter machines.

#### IV. CASE STUDY: 3-PHASE MACHINE

It has been demonstrated in Section III that multi-converter star-polygonal windings can be designed for multiphase machines. For brevity and owing to their prevalence in industry, the impact of this winding structure on machine performance will be investigated for only 3-phase machines. Thus, the proposed 24s/22p dual 3-phase machine with star-delta windings shown in Fig. 7(a) is studied in this section.

##### A. Air-gap Flux Density due to Winding MMF

The 12s/10p slot-pole number combination is a common machine topology selected owing to its high winding factor. Depending on the size and power of the machine, this combination is multiplied to obtain machines with increasing slot-pole numbers such as 24s/20p, 36s/30p and so on. This simply requires repeating the same winding layout within the same stator. Owing to its commonality, a dual 3-phase 24s/20p machine is a sensible benchmark to compare the performance of the 24s/22p dual 3-phase star-delta machine. The machine dimensions investigated in this case study are given in TABLE VI. Five machines are compared in this section to assess the cumulative impact of additional

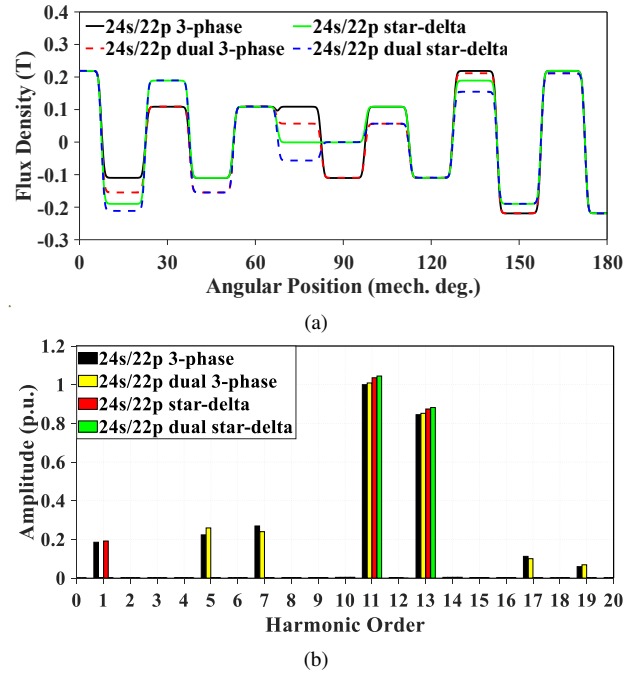


Fig. 9. Flux density comparison between different 24s/22p winding configurations with linear material conditions. (a) Air-gap flux density and (b) harmonic spectra with amplitude taken in per unit using the 24s/22p 3-phase working harmonic as reference.

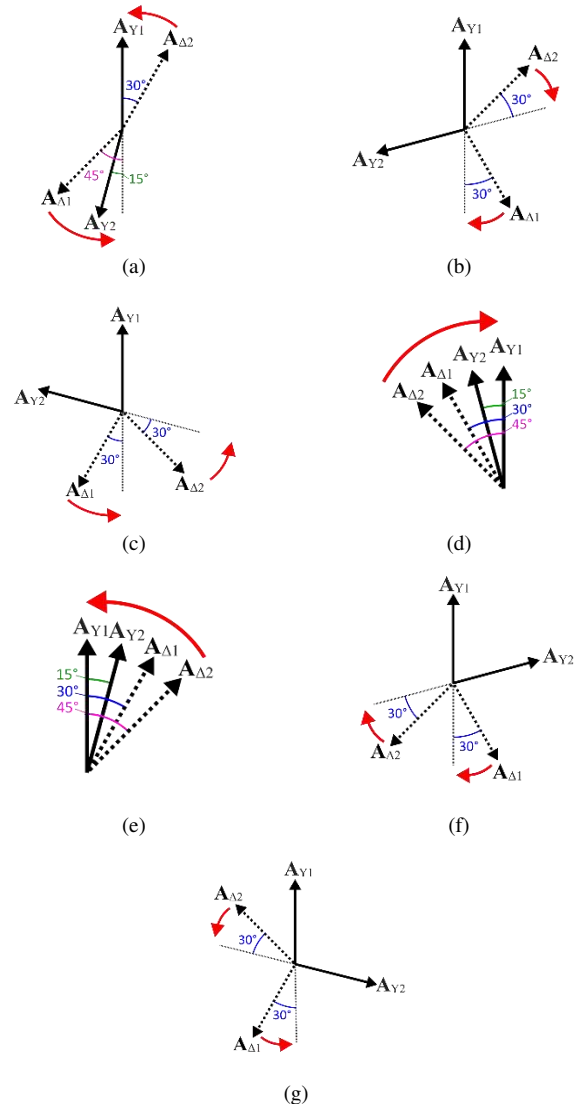


Fig. 10. Phasor diagrams for MMF harmonics in 24s/22p dual 3-phase with star-delta windings. (a) 1<sup>st</sup> harmonic, (b) 5<sup>th</sup> harmonic, (c) 7<sup>th</sup> harmonic, (d) 11<sup>th</sup> harmonic, (e) 13<sup>th</sup> harmonic, (f) 17<sup>th</sup> harmonic, and (g) 19<sup>th</sup> harmonic.

converters and star-delta windings. They are as follows: 24s/20p 3-phase, 24s/20p dual 3-phase, 24s/22p 3-phase, 24s/22p dual 3-phase, 24s/22p dual 3-phase with star-delta windings. To study the impact of each winding layout on MMF harmonics, each machine armature was excited with sinusoidal current to produce the armature flux density. These could then be plotted, and harmonic composition extracted for comparison in Fig. 11. As one would expect, in the 24s/20p machine the addition of a second converter operating at a 30° phase shift negates the 2<sup>nd</sup> order subharmonic and improves the working harmonic (10<sup>th</sup>). The 24s/22p machine is normally rich in unwanted harmonics including 1<sup>st</sup>, 5<sup>th</sup>, 7<sup>th</sup>, 17<sup>th</sup>, and 19<sup>th</sup>. The second converter operating at a 30° phase shift successfully eliminates most of these unwanted harmonics. By including star-delta windings in each of the 3-phase winding sets and then operating the second converter at a 15° phase shift, all unwanted harmonics are eliminated. Both the 11<sup>th</sup> and 13<sup>th</sup> harmonics are torque producing, and both are enhanced using this method.

### B. Torque Performance

A distinct advantage of the 24s/22p machines over the 24s/20p machines is the larger lowest common multiple (LCM) between the slot number and pole number. This leads to a greatly reduced cogging torque in the 22-pole machine, as shown in Fig. 12. It is worth noting that the cogging torque is independent of winding structure and is only dependent on the slot-pole number combinations. This is the reason why in Fig. 12, only the two slot-pole number combinations are given, not the associated winding structures. The low amplitude of the cogging torque in the 24s/22p machines will present a distinct advantage compared with the 24s/20p machine when measuring on-load torque performance. This can be seen in Fig. 13 where the machines were operated at rated current for one full electrical period, and a direct comparison of torque performance is given in TABLE VII. The on-load torque performance shows that when the machine is operated as only single  $m$ -phase, the harmonic rich MMFs contribute to substantial torque ripple. This results in a torque ripple that is greater in the 24s/22p 3-phase machine when compared with the 24s/20p 3-phase machine. After the addition of a second converter, all machines exhibit an increase in average torque and reduction in torque ripple.

To assess the overload capability of the two machines they were operated with increasing phase current up to 3 times the rated amount. Fig. 14 shows that the 24s/22p machine achieves higher torque for currents within the normal operating region but has a lower overload capability at higher phase currents as its torque performance diminishes when compared with the 24s/20p dual 3-phase machine. However, for all values of supplied phase current the torque ripple of the 24s/22p dual star-delta machine remains less than the 24s/20p dual 3-phase machine.

### C. Flux Weakening

To evaluate the capacity for flux weakening in both machines they were each spun at rated speed for one electrical period while being supplied with a range of negative  $d$ -axis currents. The current at which the phase voltage reduces to zero serves as an indicator showing the maximum flux weakening capability. However, as there is no neutral point

TABLE VI PROPOSED 3-PHASE MACHINE SPECIFICATIONS

Slot number	24	Stack length (mm)	50
Pole number	20/22	Air-gap length (mm)	1
Rated current ( $A_{rms}$ )	7.34	Tooth width (mm)	3.5
Rated speed (RPM)	400	Tooth height (mm)	2.5
Turns per phase	132/66	Stator yoke height (mm)	3.7
Stator outer radius (mm)	50	Magnet thickness (mm)	3
Rotor outer radius (mm)	27.5	Magnet remanence (T)	1.24

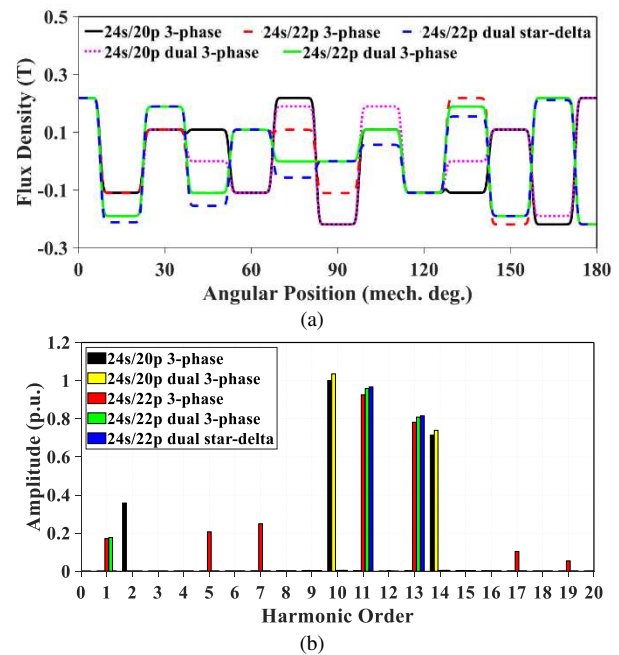


Fig. 11. Air-gap flux density due to armature windings. (a) 24-slot waveforms and (b) 24-slot spectra.

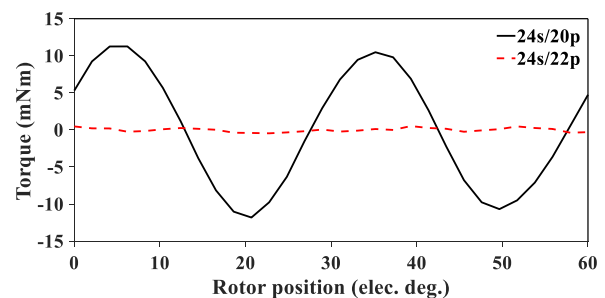


Fig. 12. Cogging torque comparison of two slot-pole combinations for 3-phase machines.

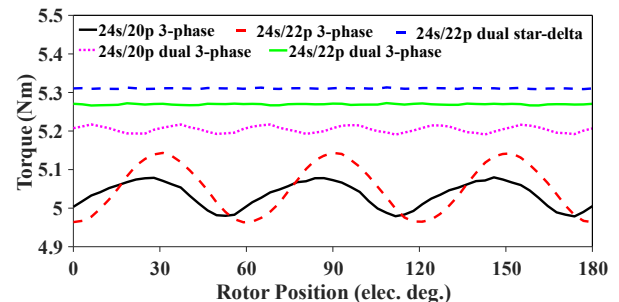


Fig. 13. Torque performance comparison for investigated machines.

TABLE VII TORQUE PERFORMANCE OF INVESTIGATED 3-PHASE MACHINES

Winding Type	Average Torque (Nm)	Torque Ripple (Nm)
24s/20p 3-phase	5.03	0.103 (2.04%)
24s/20p dual 3-phase	5.20 (+3.38%)	0.0269 (0.517%)
24s/22p 3-phase	5.05 (+0.40%)	0.180 (3.56%)
24s/22p dual 3-phase	5.27 (+4.77%)	0.0063 (0.119%)
24s/22p dual 3-phase star-delta	5.31 (+5.57%)	0.0047 (0.088%)

Note: torque ripple is the peak-to-peak torque.

in the 24s/22p dual star-delta machine, it is not possible to measure phase voltage. Thus, the line voltage was used for both machines and the results for this investigation can be seen in Fig. 15. The 24s/22p dual star-delta wound machine exhibits greater flux weakening capability evidenced by the reduction of line voltage to zero at 9.3A, as opposed to 10.8A for the 24s/20p dual 3-phase machine. This means that the 24s/22p dual star-delta machine can achieve greater flux weakening with a comparatively lower current compared to the 24s/20p dual 3-phase machine. This suggests that the dual star-delta winding holds promise for applications demanding a broad speed range, such as electric vehicles.

#### D. Loss Analysis

The elimination of unwanted MMF harmonics is known to be able to reduce losses, especially in the rotor. Therefore, the losses for each machine had to be calculated during operation. For the hysteresis and eddy current losses in the stator, the two-term Steinmetz equation was used

$$P_{stator} = K_h f B^2 + K_e f^2 B^2 \quad (17)$$

where  $K_h$  and  $K_e$  are the hysteresis and eddy current loss coefficients respectively,  $f$  is the frequency of the rotating PM field, and  $B$  is the magnitude of the flux density. It is worth noting that a solid rotor was used to mimic the case of a direct drive wind power generator, so only eddy current losses in the rotor and PMs were calculated. This was done by summing the power loss in each mesh element using

$$P_{eddy\ current} = \sum_{i=1}^K \frac{J_i^2 A_i}{\sigma_c} \quad (18)$$

where  $J$  and  $A$  are the current density and area of the mesh element, respectively,  $\sigma_c$  is the conductivity of the material, and  $K$  is the total number of mesh elements. Finally, in the windings only copper losses caused by coil DC resistance were accounted for and were calculated using

$$P_{copper} = N_s N_c^2 \rho \frac{L_w}{S k_b} I_{rms}^2 \quad (19)$$

where  $N_s$  is the number of slots,  $N_c$  is the number of conductors per slot,  $\rho$  ( $\Omega\text{m}$ ) is the resistivity of copper at room temperature,  $L_w$  (m) is the sum of both active winding length and end winding length,  $S$  ( $\text{m}^2$ ) is the slot area,  $k_b$  is the slot packing factor, and  $I_{rms}$  (A) is the RMS phase current. These losses are then compared and summed to give an idea of machine efficiency, as evidenced in TABLE VIII. These results show that the 24s/22p dual 3-phase machine with star-delta windings exhibits the highest efficiency of all 3-phase machines investigated. An important note comes from the comparison of the 24s/22p dual 3-phase machine with and without star-delta windings, in the star-delta wound machine the rotor losses have been substantially reduced. This is owing to the successful elimination of the 1<sup>st</sup> parasitic subharmonic which can only be achieved through the combination of dual 3-phases and star-delta windings.

#### V. EXPERIMENTAL RESULTS

To validate the simulations in this paper, a 24-slot/22-pole dual 3-phase machine with star-delta windings was

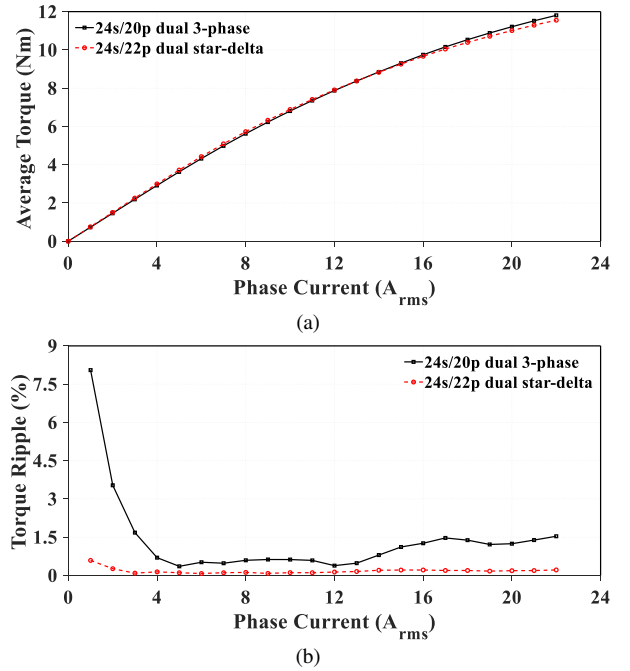


Fig. 14. Torque performance comparison with increasing phase current. (a) Onload torque, and (b) torque ripple coefficient.

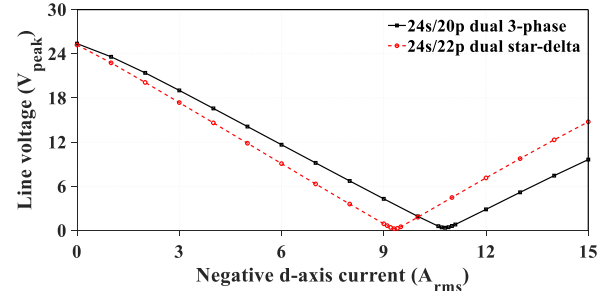


Fig. 15. Impact of negative  $d$ -axis current on line voltage.

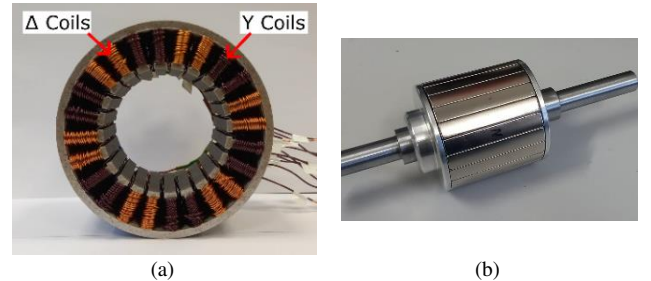


Fig. 16. Dual 3-phase star-delta winding prototype machine. (a) stator with winding layout and (b) 22-pole rotor.

manufactured, as shown in Fig. 16. The specifications of this machine can be found in TABLE VI, albeit with slightly reduced magnet size to account for manufacturing tolerance.

#### A. EMF Measurements

The prototype machine was spun at rated speed to obtain waveforms for open-circuit EMF. As there is no neutral point, the phase voltages could not be obtained, thus the open-circuit voltages of star and delta coils were measured in addition to the line EMF. The measured results are compared with simulation results, as shown in Fig. 17, and a good

TABLE VIII LOSS COMPARISON BETWEEN INVESTIGATED 3-PHASE MACHINES

Winding Type	Stator Loss (W)	Rotor Loss (mW)	PM Loss (mW)	Copper Loss (W)	Efficiency (%)
24s/20p 3-phase	4.59	128	10.9	47.1	75.40
24s/20p dual 3-phase	4.46 (-2.83%)	19.4 (-84.84%)	10.3 (-5.50%)	47.1	76.32 (+1.21%)
24s/22p 3-phase	4.97 (+8.28%)	96.6 (-24.53%)	14.3 (+31.19%)	47.1	75.33 (-0.09%)
24s/22p dual 3-phase	4.69 (+2.18%)	86.2 (-32.66%)	14.8 (+35.78%)	47.1	76.49 (+1.45%)
24s/22p dual 3-phase star-delta	4.78 (+4.14%)	15.5 (-87.89%)	14.6 (+33.94%)	47.1	76.66 (+1.67%)

agreement can be seen in all cases. The fundamental EMF of the measured delta coil and star coil is reduced by 4.9% and 4.2% respectively when compared to the simulation results. This yields an overall reduction in the line EMF fundamental by 4.5%. After consideration of manufacturing tolerance, i.e., slightly reduced magnets and unaccounted stacking factor, this minor reduction is within the acceptable range.

### B. Static Torque Measurements

Following the method outlined in [30], a couple of static torque measurements were carried out to validate the torque performance of the prototype dual star-delta winding machine, using the test rig shown in Fig. 18(a). This method can be used for both cogging torque and static torque. Due to the small scale of the prototype machine and the machine periodicity, the amplitude of the expected cogging torque is less than 1mNm. The margin for error on rotor position coupled with ‘noise’ in the measurement apparatus made obtaining any cogging torque waveform impossible. However, static onload torque could be easily measured. Using a dual DC power supply to supply the two 3-phase windings such that  $I_{A1} = I_{A2} = I$ ,  $I_{B1} = I_{B2} = I_{C1} = I_{C2} = -I/2$ , where  $I$  is the DC current, the static torque of the machine rotated through 360 elec. deg. could be measured, as shown in Fig. 18(b). In addition to this, the peak static torque could be measured at 90 elec. deg. phase angle (equivalent to the  $q$ -axis) across increasing phase currents, as shown in Fig. 18(c). As with the EMF measurements, there is a good agreement between the simulated and measured results. However, there is a 4.0% reduction in the amplitude of the static torque across rotor position, and the mean percentage reduction of peak static torque for increasing phase currents is 3.9%. Again, the reduction in torque amplitude in both experiments is mainly due to the manufacturing tolerance and is therefore deemed acceptable as validation for the prototype machine.

## VI. CONCLUSION

In this paper a general method for the identification and design of  $m$ -phase,  $n$ -converter machines with star-polygonal windings has been developed. Tables can be generated for any  $m$ -phase machine supplied by  $n$ -converters that are feasible and promising opportunities to employ combined star-polygonal windings for harmonic elimination. These tables include solutions that employ a wide range of coil pitches, and in this work two cases are investigated. When the coil pitch is 1, machines with star-polygonal windings achieve higher torque, reduced torque ripple, and higher efficiency than non star-polygonal connected machines of similar design. This is particularly useful as it maintains the advantage of short end windings inherent to concentrated windings, while also drastically reducing the rotor losses that come about from this structure.

A 24s/22p dual star-delta wound machine was compared with a 24s/20p dual 3-phase machine. FEA results demonstrated it achieved a higher average torque (5.31Nm vs 5.2Nm), reduced torque ripple (0.088% vs 0.517%), greater machine efficiency (76.66% vs 76.32%), and enhanced flux weakening capability. A prototype machine was manufactured and both EMF and static torque measurements closely match the simulation results, corroborating the expected performance of the 24-slot 22-pole machine with dual 3-phase star-delta windings.

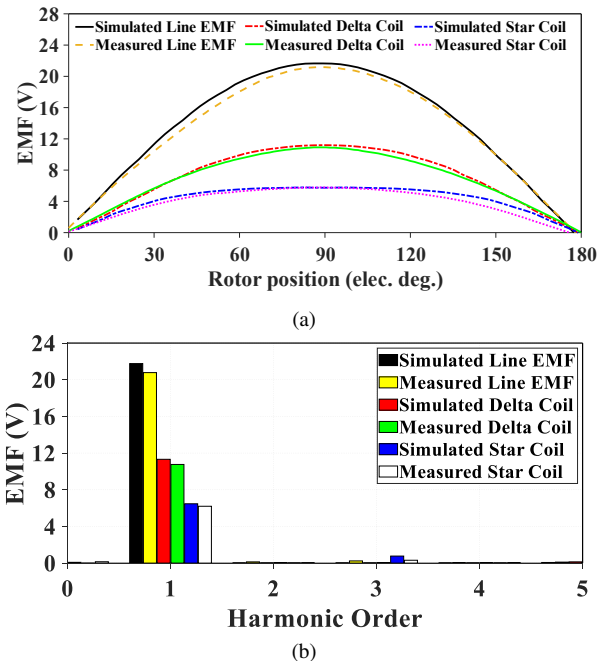


Fig. 17. Star and delta coil as well as line EMFs of dual 3-phase star-delta winding prototype machine. (a) Waveforms, and (b) spectra.

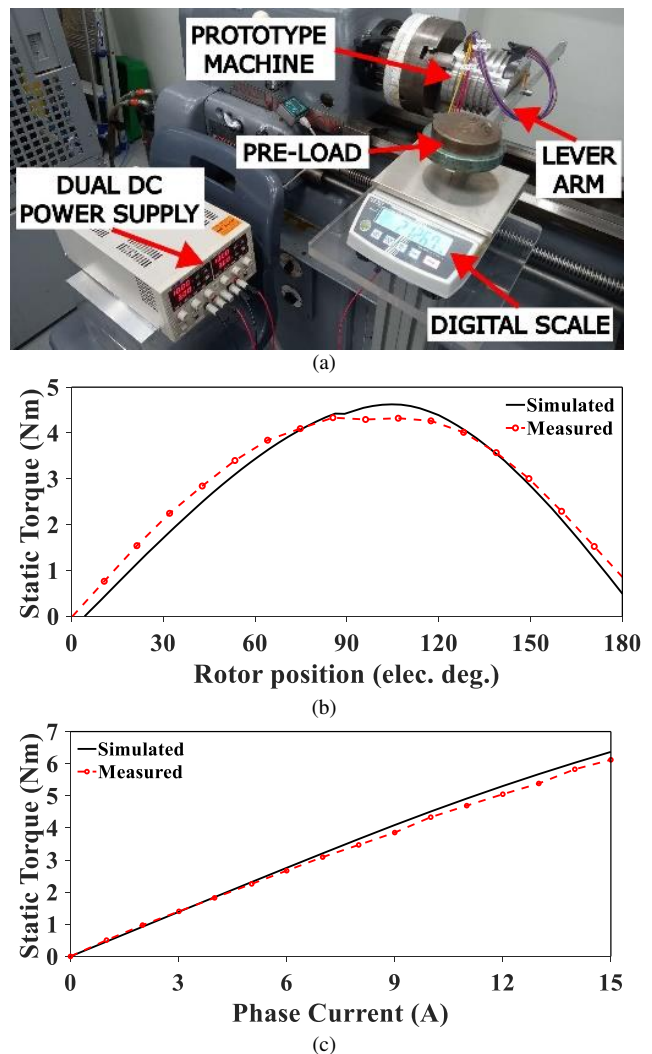


Fig. 18. Measured and simulated static torques. (a) Experimental setup, (b) static torque vs current phase angle, and (c) peak static torque (at 90 elec. deg.) vs increasing phase current.

## ACKNOWLEDGMENT

This work is supported by the UK EPSRC Prosperity Partnership "A New Partnership in Offshore Wind" under Grant No. EP/R004900/1.

For the purpose of open access, the author has applied a Creative Commons Attribution (CC BY) licence to any Author Accepted Manuscript version arising.

## REFERENCES

- [1] A. Pami, H. Teresa, K. Sarah, and K. Matti, "Chapter 1 - introduction: Electrification and the energy transition," in *Electrification: Accelerating the energy transition*, 2021, pp. 3-24.
- [2] A. M. El-Refaie, "Fractional-slot concentrated-windings synchronous permanent magnet machines: Opportunities and challenges," *IEEE Trans. Ind. Electron.*, vol. 57, no. 1, pp. 107-121, Jan. 2010.
- [3] J. Cros and P. Viarouge, "Synthesis of high performance pm motors with concentrated windings," *IEEE Trans. Energy Convers.*, vol. 17, no. 2, pp. 248-253, June 2002.
- [4] N. Bianchi, S. Bolognani, M. D. Pre, and G. Grezzani, "Design considerations for fractional-slot winding configurations of synchronous machines," *IEEE Trans. Ind. Appl.*, vol. 42, no. 4, pp. 997-1006, July 2006.
- [5] D. Ishak, Z. Q. Zhu, and D. Howe, "Comparative study of permanent magnet brushless motors with all teeth and alternative teeth windings," presented at the Second IEE International Conference on Power Electronics, Machines and Drives, Edinburgh, UK, Mar., 2004.
- [6] D. Ishak, Z. Q. Zhu, and D. Howe, "Analytical prediction of rotor eddy current losses in permanent magnet brushless machines with all teeth and alternate teeth windings—part i: Polar co-ordinate model," presented at the ICEMS, Lodz, Poland, Sept., 2004.
- [7] Z. Q. Zhu, D. Ishak, and D. Howe, "Analytical prediction of rotor eddy current losses in permanent magnet brushless machines with all teeth and alternate teeth windings—part ii: Rectangular co-ordinate model," presented at the ICEMS, Lodz, Poland, Sept., 2004.
- [8] P. B. Reddy, K.-K. Huh, and A. M. El-Refaie, "Generalized approach of stator shifting in interior permanent-magnet machines equipped with fractional-slot concentrated windings," *IEEE Trans. Ind. Electron.*, vol. 61, no. 9, pp. 5035-5046, Sept. 2014.
- [9] A. S. Abdel-Khalik, S. Ahmed, and A. M. Massoud, "Effect of multilayer windings with different stator winding connections on interior pm machines for ev applications," *IEEE Trans. Magn.*, vol. 52, no. 2, pp. 1-7, Feb. 2016.
- [10] X.-Y. Sun, Z.-Q. Zhu, and L. Xu, "Analysis of excitation winding induced emf in non-overlapped stator wound field synchronous machines," *IEEE Trans. Energy Convers.*, vol. 37, no. 1, pp. 685-695, Mar. 2022.
- [11] Z. Q. Zhu, Y. J. Zhou, J. T. Chen, and J. E. Green, "Investigation of nonoverlapping stator wound-field synchronous machines," *IEEE Trans. Energy Convers.*, vol. 30, no. 4, pp. 1420-1427, Dec. 2015.
- [12] Z. Zhu, S. Wang, B. Shao, L. Yan, P. Xu, and Y. Ren, "Advances in dual-three-phase permanent magnet synchronous machines and control techniques," *Energies*, vol. 14, no. 22, p. 7508, Nov. 2021.
- [13] M. Barcaro, N. Bianchi, and F. Magnussen, "Analysis and tests of a dual three-phase 12-slot 10-pole permanent magnet motor," in *2009 IEEE Energy Conversion Congress and Exposition*, Sept. 2009: IEEE.
- [14] V. I. Patel, J. Wang, W. Wang, and X. Chen, "Six-phase fractional-slot-per-pole-per-phase permanent-magnet machines with low space harmonics for electric vehicle application," *IEEE Trans. Ind. Appl.*, vol. 50, no. 4, pp. 2554-2563, July 2014.
- [15] A. S. Abdel-Khalik, S. Ahmed, and A. M. Massoud, "A six-phase 24-slot/10-pole permanent-magnet machine with low space harmonics for electric vehicle applications," *IEEE Trans. Magn.*, vol. 52, no. 6, pp. 1-10, June 2016.
- [16] Z. Wu, Z. Q. Zhu, and C. Wang, "Reduction of on-load dc winding-induced voltage in partitioned stator wound field switched flux machines by dual three-phase armature winding," *IEEE Trans. Ind. Electron.*, vol. 69, no. 6, pp. 5409-5420, July 2022.
- [17] K. S. Garner and M. J. Kamper, "Reducing mmf harmonics and core loss effect of non-overlap winding wound rotor synchronous machine (wrsm)," in *2017 IEEE Energy Conversion Congress and Exposition (ECCE)*, Oct. 2017: IEEE.
- [18] E. Fornasiero, N. Bianchi, and S. Bolognani, "Slot harmonic impact on rotor losses in fractional-slot permanent-magnet machines," *IEEE Trans. Ind. Electron.*, vol. 59, no. 6, pp. 2557-2564, June 2012.
- [19] A. S. Abdel-Khalik, S. Ahmed, and A. M. Massoud, "Low space harmonics cancellation in double-layer fractional slot winding using dual multiphase winding," *IEEE Trans. Magn.*, vol. 51, no. 5, pp. 1-10, May 2015.
- [20] W. Zhao, J. Zheng, J. Ji, S. Zhu, and M. Kang, "Star and delta hybrid connection of a fscw pm machine for low space harmonics," *IEEE Trans. Ind. Electron.*, vol. 65, no. 12, pp. 9266-9279, Dec. 2018.
- [21] S. Sadeghi, L. Guo, H. A. Toliyat, and L. Parsa, "Wide operational speed range of five-phase permanent magnet machines by using different stator winding configurations," *IEEE Trans. Ind. Electron.*, vol. 59, no. 6, pp. 2621-2631, June 2012.
- [22] A. Mohammadpour, S. Sadeghi, and L. Parsa, "A generalized fault-tolerant control strategy for five-phase pm motor drives considering star, pentagon, and pentacle connections of stator windings," *IEEE Trans. Ind. Electron.*, vol. 61, no. 1, pp. 63-75, Jan. 2014.
- [23] B. Zhao, J. Gong, T. Tong, Y. Xu, E. Semail, N.-K. Nguyen, and F. Gillon, "A novel five-phase fractional slot concentrated winding with low space harmonic contents," *IEEE Trans. Magn.*, vol. 57, no. 6, pp. 1-5, June 2021.
- [24] M. S. Islam, M. A. Kabir, R. Mikail, and I. Husain, "Space-shifted wye-delta winding to minimize space harmonics of fractional-slot winding," *IEEE Trans. Ind. Appl.*, vol. 56, no. 3, May 2020.
- [25] I. A. Rudden, G. J. Li, D. K. Kana, Z. Q. Zhu, A. Duke, R. Clark, and A. Thomas, "Space harmonic cancellation in a dual three-phase spm machine with star-delta windings," *IEEE Trans. Energy Convers.*, pp. 1-10, July 2023.
- [26] J. Yu, J. Yang, S. Dai, Z. Wang, Q. Li, S. Huang, and S. Huang, "Investigation on performance of multiple three-phase electrical machine with star-delta windings," *IEEE Trans. Ind. Electron.*, pp. 1-11, Oct. 2023.
- [27] N. Bianchi and M. D. Pre, *Use of the star of slots in designing fractional-slot single-layer synchronous motors* (Proc. Inst. Elect. Eng.—electr. Power appl). 2006.
- [28] Z. Q. Zhu and Y. Liu, "Analysis of air-gap field modulation and magnetic gearing effect in fractional-slot concentrated-winding permanent-magnet synchronous machines," *IEEE Trans. Ind. Electron.*, vol. 65, no. 5, pp. 3688-3698, May 2018.
- [29] Y. Liu and Z. Q. Zhu, "Influence of gear ratio on the performance of fractional slot concentrated winding permanent magnet machines," *IEEE Trans. Ind. Electron.*, vol. 66, no. 10, pp. 7593-7602, Oct. 2019.
- [30] Z. Q. Zhu, "A simple method for measuring cogging torque in permanent magnet machines," in *IEEE Power & Energy Society General Meeting*, July 2009: IEEE.